Thermodynamics of Electron Transfer in Oxygenic Photosynthetic Reaction Centers: A Pulsed Photoacoustic Study of Electron Transfer in Photosystem I Reveals a Similarity to Bacterial Reaction Centers in both Volume Change and Entropy†

Jian-Min Hou,‡ Vladimir A. Boichenko,‡,§ Ying-Chun Wang,|| Parag R. Chitnis,|| and David Mauzerall*,‡

The Rockefeller University, 1230 York Avenue, New York, New York 10021, Institute of Basic Biological Problems, Russian Academy of Sciences, Pushchino 142290, Russia, and Department of Biochemistry, Biophysics and Molecular Biology, Iowa State University, Ames, Iowa 50010

Received August 31, 2000; Revised Manuscript Received April 19, 2001

ABSTRACT: The thermodynamic properties of electron transfer in biological systems are far less known in comparison with that of their kinetics. In this paper the enthalpy and entropy of electron transfer in the purified photosystem I trimer complexes from *Synechocystis* sp. PCC 6803 have been studied, using pulsed time-resolved photoacoustics on the 1 μs time scale. The volume contraction of reaction centers of photosystem I, which results directly from the light-induced charge separation forming $P_{700}^{+}F_A/F_B^{-}$ from the excited-state P_{700}*, is determined to be -26 ± 2 Å^3. The enthalpy of the above electron-transfer reaction is found to be -0.39 ± 0.1 eV. Photoacoustic estimation of the quantum yield of photochemistry in the purified photosystem I trimer complex showed it to be close to unity. Taking the free energy of the above reaction as the difference of their redox potentials in situ allows us to calculate an apparent entropy change ($T\Delta S$) of $+0.35 \pm 0.1$ eV. These values of ΔV and $T\Delta S$ are similar to those of bacterial reaction centers. The unexpected sign of entropy of electron transfer is tentatively assigned, as in the bacterial case, to the escape of counterions from the surface of the particles. The apparent entropy change of electron transfer in biological system is significant and cannot be neglected.

The kinetics and thermodynamics of electron transfer in a biological system are two equally important issues for the understanding of the electron-transfer mechanisms. During the past decade the kinetics of electron-transfer steps in reaction centers of anoxygenic and oxygenic photosynthesis has been thoroughly investigated over the complete time scale of femtosecond to second (see reviews in refs *1*−*4*). These studies have established the main pathways and kinetics of electron transfer in the bacterial reaction centers, photosystem (PS)[1] I and PS II. PS I is a pigment−protein complex embedded in the photosynthetic membranes of oxygenic photosynthetic organisms. It drives electron transfer from reduced plastocyanin (or cytochrome c_6) to oxidized ferredoxin (or flavodoxin) to generate NADPH (*5*, *6*). Recent X-ray crystallographic analysis of cyanobacterial PS I from *Synechococcus elongatus* at 4 Å resolution has revealed its structure and overall organization (*7*). It is widely accepted that the electron transport chain of PS I comprises the primary electron donor P_{700} and five electron acceptors: the primary electron acceptor A_0 (Chl *a*), the secondary acceptor A_1 (phylloquinone or vitamin K), the tertiary acceptor F_X (an iron−sulfur complex), and the similar terminal acceptors F_A and F_B . Upon excitation of P_{700} to its lowest excited singlet state (P_{700}*), an electron is transferred to A_0 and further to A_1 on the picosecond time scale, then further to F_X, and finally to F_A and/or F_B on the nanosecond time scale.

In contrast to the knowledge of the kinetics, that of the thermodynamics of electron-transfer steps in photosynthesis, such as volume change, enthalpy, and entropy, is far less well-known (*8*). The free energy of the electron-transfer process is obtained from midpoint redox potentials of the respective components or from the analysis of kinetic data (*9*, *10*). The pulsed photoacoustic (PA) method provides direct measurement of the enthalpy change of photosynthetic reactions (*11*−*13*). A gas-coupled microphone in a closed chamber was used as a detector on the millisecond time scale. This method allowed in vivo measurements of the photosynthetic thermal efficiency (TE), or energy storage, and optical cross section of the light harvesting systems (*14*−*17*). The use of piezoelectric films acoustically coupled to a liquid sample and a pulsed laser light source increased the time resolution of the PA technique to the nanosecond time

† This work is supported by grants from the NSF (MCB 99-04522) and NIH (GM 25693).

* Corresponding author. E-mail: mauzera@rockvax.rockefeller.edu. Fax: (212) 327-8853.

‡ The Rockefeller University.

§ Russian Academy of Sciences.

|| Iowa State University.

[1] Abbreviations: Asc, sodium ascorbate; Chl, chlorophyll; DAD, diaminodurene or 2,3,5,6-tetramethyl-*p*-phenylenediamine; DCIP, dichloro-2,6-phenolindophenol; DM, dodecyl β-D-maltoside; Hepes, *N*-(2-hydroxyethyl)piperazine-*N*′-2-ethanesulfonic acid; MV, methyl viologen; PA, photoacoustic(s); PMS, phenazine methosulfate; PS, photosystem; PTRPA, pulsed time-resolved photoacoustics; TE, thermal efficiency; TMPD, *N*,*N*,*N*′,*N*′-tetramethyl-*p*-phenylenediamine.

10.1021/bi0103720 CCC: $20.00
Published on Web 05/23/2001

scale (*18*−*21*). This pulsed, time-resolved photoacoustic methodology (PTRPA) enables one to determine both the volume change and enthalpy of photobiological reactions (*11*, *22*). There are earlier PA thermodynamic studies of isolated photosynthetic reaction centers from bacteria *Rhodobacter sphaeroides* (*23*−*25*), PS I from cyanobacteria (*26*−*27*), and PS II from spinach and *Chlamydomomas reinhardtii* (*26*).

Theoretical calculations of electron transfer have often assumed the reaction entropy to be zero. For example, the standard formulation of Marcus theory assumed that the vibrations coupled to electron transfer have the same frequency in reactant and product states (*28*). Treatments of the temperature dependence of the rate of electron transfer often assume that the free energy is independent of temperature (*29*, *30*). These simplifications are used to define the rate of the majority of intraprotein electron-transfer reactions. However, these assumptions are put into question by recent work. By use of PTRPA we have measured the volume change, the enthalpy, and thus, knowing the free energy, the entropy of electron transfer in aqueous solution (*31*) and in the photosynthetic reaction center complex of *Rb. sphaeroides* (*32*). A significant entropy of electron transfer in both aqueous solution and protein complex was found. Therefore, it is of importance to study other photosynthetic reaction centers to provide further evidence for this neglected entropy of electron transfer.

In this work PTRPA was used to obtain the thermodynamic parameters of the flash-induced electron-transfer reaction in the purified PS I complex from the cyanobacterium *Synechocystis* PCC 6803. These data provide evidence of significant entropy and volume changes on electron transfer in the PS I complex.

MATERIALS AND METHODS

Preparation of the PS I Reaction Center. PS I trimer complexes were prepared according to published methods (*33*). *Synechocystis* sp. PCC 6803 cells were grown in BG-11 medium under 40 μE m^{-2} s^{-1} light intensity at 30 °C. Cells were collected at the logarithmic growth phase and centrifuged at 5000*g*. Pellets were resuspended in 50 mM MOPS (pH 7.0), 10 mM NaCl, and 0.4 M sucrose and stored at −20 °C until further use. The cells were thawed at room temperature and broken in a bead beater (Biospec Products) in the presence of the protease inhibitor 0.2 mM phenylmethanesulfonyl fluoride. Unbroken cells were removed by centrifugation at 5000*g* for 30 min at 4 °C, and the membranes were pelleted by centrifugation at 50000*g* for 1 h at 4 °C and resuspended in 50 mM MOPS (pH 7.0), 10 mM NaCl, and 0.4 M sucrose. PS I trimer complexes were isolated by solubilizing the membranes with DM (final concentration of 1.5%) for 30 min at room temperature and sucrose gradient (10−30%) ultracentrifugation at 160000*g* overnight in 10 mM MOPS (pH 7.0) and 0.05% DM. The storage medium containing a high concentration of sucrose was replaced by the suspending medium (10 mM buffer) for PA measurements using Centriprep (Amicon).

The Chl concentrations of PS I trimer complexes were measured by extraction with 80% (v/v) acetone. P_{700} was estimated by the measurement of absorption changes at 700 nm induced by chemical oxidation and reduction (*33*). The ratio of Chl to P_{700} was determined to be 80 ± 7.

Photoacoustic Measurements. The procedures of the pulse time-resolved photoacoustics are similar to the methodology described elsewhere (*31*). A Nd:YAG laser and OPO were used to produce light of 625 and 680 nm in a homemade photoacoustic apparatus with 1 mm light path. The PA detector is a 128 μm piezoelectric film following a dielectric mirror (>99% reflection, Newport) according to the design of Arnaut et al. (*34*). The voltage produced by the piezoelectric film was amplified (typical gain 1000) and filtered (Ithaco 1201). The signal was digitized with a Tektronix RTD 710 or DPS 520C and read into the computer (HP 340). The PA signal and light energy were measured in batches of 32. The temperature was controlled to ±0.1 °C and was simultaneously recorded by a thermocouple in the PA cell. The Higgins carbon black ink (Eberbard Faber) and the jet black ink (Sheaffer) were used as the external PA reference.

Global analysis is based on the nonlinear least-squares fit of all of the measurements by reiterative convolution at different temperatures and different excitation energy to obtain the thermodynamic parameters of the reaction centers of PS I.

THEORY

Quantum Yield of Photochemistry. The PA measurement provides the enthalpy or volume changes times the quantum yield, and thus this yield must be known to obtain the enthalpy and volume changes.

The light saturation function at 4 °C (where there is no thermal signal; see below) contains the photophysical quantum yield (*35*). This refers to that fraction of absorbed light in a unit of optical cross section (σ) that excites the reaction of interest. For a simple system with one cross section and immediate recovery following a failed hit, the PA signal is described by the cumulative one-hit Poisson distribution:

$$\mathrm{PA} = N\mathrm{PA}_0(1 - \mathrm{e}^{-\sigma\Phi E}) \quad (1)$$

$$E = E_0(1 - 10^{-A}) \quad (2)$$

where N is the number of centers in the sample, PA_0 is the photoacoustic signal produced per successful hit of the reaction centers, σ and $\Phi\sigma$ are the optical cross section and effective optical cross section, Φ is the quantum yield, E_0 is the incident excitation photon flux, E is the photon energy absorbed by the sample, and A is the absorbency per 2 mm of solution (1 mm cell and mirror).

The optical cross section, σ, with units of area per reaction center, can be calculated from the absolute absorption spectra of the sample, the chlorophyll content, and ratio of chlorophyll to the primary electron donor P_{700}.

We assume E is uniform and constant across the sample; i.e., the sample is optically thin with $A \leq 0.1$. Then a correction can be made by the equation:

$$E = E_0 \times 2.3A \quad (3)$$

Recovery Time of Reaction Centers. Since the signals are weak and averaging is required, the recovery time of the preparation must be measured to ensure that the centers have returned to their initial state before the next actinic pulse. This recovery time (τ) can be measured by varying the

frequency of *n* saturating flashes and measuring the average PA signal. Allowing for fast and slow recovery:

$$PA = PA_0[a + (1 - a)(1 - e^{-\Delta t/\tau})] \quad (4)$$

where PA_0 is the maximum PA signal, Δt is time between the flashes, τ is the recovery time of the samples, a is the fraction of the fast recovery component, and $(1 - a)$ is the fraction of the τ component.

Volume Change. There are two different ways to obtain the volume change of the reaction centers: (1) volume yield method and (2) saturation method.

(1) Linear Volume Yield Method. A reference compound, which degrades all of the absorbed photons to heat in less than the resolution time of the apparatus and with the same absorbency at the excitation wavelength as the sample, is used to calibrate the system. The photoacoustic signal from the reference is

$$PA_{ref} = \frac{F\alpha'}{\kappa} EI(t) \quad (5)$$

where F is the piezo film sensitivity, α' is the thermal expansivity (α)/heat capacity $\times$ density, κ is the compressibility, E is the photon energy absorbed by the sample, and $I(t)$ is the impulse response of the system.

If the PA signal from the reaction centers contains only fast components [i.e., responds as $I(t)$]:

$$PA_{RC} = \frac{F}{\kappa}[\alpha' Q_{RC} + \Delta V_{RC}]I(t) \quad (6)$$

where Q_{RC} is the heat output which includes the enthalpy change of the reaction and other rapidly released heat and ΔV_{RC} is the volume change of the reaction. In the magic solvent, water, one easily separates the thermal and volume signals. The thermal signal disappears at the temperature of maximum density of the suspending medium, T_m, near 4 °C, where $\alpha = 0$, leaving the volume term only. Assuming ΔV does not change over the small temperature range, ΔV_{RC} is obtained in the limiting low pulse energy region (linear region of eq 8) by normalizing to the reference PA signal, conversion of PA_{ref} to volume by α' at 25 °C, and correcting for the change in compressibility of water between T_m and 25 °C:

$$\Delta V_{RC} = \frac{PA_{RC}^{Tm}}{PA_{ref}^{25}} \frac{\kappa^{T_m}}{\kappa^{25}} \Delta V_{ref} \quad (7)$$

where $\Delta V_{ref} = \alpha' E$ is the thermal volume change of the reference at its temperature. Since the system is linear, one can calculate ΔV_{ref}, the thermal volume change at 25 °C for each absorbed photon at the excitation wavelength, 18 Å^3 at 680 nm and 19.6 Å^3 at 625 nm. At low energy one obtains the yield per center ΔV_y multiplied by the quantum yield:

$$\Delta V_{RC} = N\Delta V_y \frac{(1 - e^{-\Phi\sigma E})}{N\sigma E} \approx \Delta V_y \Phi \text{ (at low E)} \quad (8)$$

(2) Saturation Excitation Photon Flux Method. At finite excitation photon flux, the observed ΔV decreases because of saturation. Fitting of the data to eq 9 allows one to obtain the real volume change ΔV_s:

$$\Delta V_{RC} = N\Delta V_s(1 - e^{-\Phi\sigma E}) \approx N\Delta V_s \text{ (at high E)} \quad (9)$$

Now one must calculate the number of reaction centers in the illuminated volume of the cell, N, to obtain the real volume change ΔV_s. This is obtained from the total Chl concentration and the number of Chls per reaction center. Note that this method involves no assumptions concerning quantum yield, only that with sufficient energy all centers are successfully "hit". Thus agreement with the volume yield method proves that the photophysical quantum yield is unity.

Thermal Efficiency and Enthalpy. Assuming ΔV is constant, subtraction from PA_{RC} at 25 °C gives the heat release (eq 6). Subtraction of the heat released between the excitation energy and that of the trap then gives the heat of reaction. The enthalpy is the negative of this heat. In our experiments to maximize signal to noise we use the ratio of the slopes $d(PA\kappa)/d\alpha$ for RC and for reference ink over the range of 4−25 °C (enthalpy ΔH in eq 10, thermal efficiency TE in eq 11):

$$\Delta H = (E_{h\nu} - E_{trap}) - \frac{\left(\frac{d(PA\kappa)_{RC}}{d\alpha}\right)}{\left(\frac{d(PA\kappa)_{ref}}{d\alpha}\right)} E_{h\nu} \quad (10)$$

$$TE = 1 - \frac{\left(\frac{d(PA\kappa)_{RC}}{d\alpha}\right)}{\left(\frac{d(PA\kappa)_{ref}}{d\alpha}\right)} \frac{E_{h\nu}}{E_{trap}} + \frac{E_{h\nu} - E_{trap}}{E_{trap}} \quad (11)$$

Similar to the volume change yield, the thermal efficiency varies with the flash energy:

$$TE = TE_0 \frac{(1 - e^{-\Phi\sigma E})}{\sigma E} \quad (12)$$

RESULTS

Photoacoustic Signals. Figure 1 shows the typical photoacoustic wave from the purified PS I trimer complexes of *Synechocystis* 6803. Upon excitation of the reaction centers with a weak pulse of 680 nm light at 25 °C, a negative photoacoustic signal is observed (Figure 1, curve 4) in contrast to that of the reference or light saturation PS I at 25 °C, which has a positive amplitude (Figure 1, curves 1 and 2). The observed negative signal of PS I contains two components, volume change and heat release (eq 6).

To ensure our data, we use two kinds of references. A reference is a sample, which degrades all absorbed energy to heat within the resolving time of the apparatus. One is an external reference (*13*, *18*) (Figure 1, curve 1), carbon ink, the other is an internal reference, i.e., the light-saturated PS I reaction center without addition of electron acceptors or donors (Figure 1, curve 2). These two types of references show very good agreement. At room temperature they have identical amplitude (±3%) and shape. At ~4 °C the PA signals of both are zero.

PS I complexes show a large negative amplitude at 25 °C and one even larger at 4 °C (Figure 1, curves 4 and 5). This demonstrates that the PA signal contains a volume contrac-

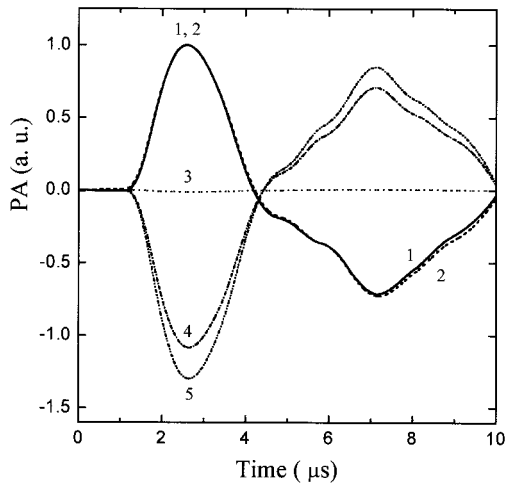

FIGURE 1: PA signal of PS I trimer complexes and reference ink: OD_{680} = 0.178/mm, 10 mM Hepes, 0.03% DM, pH 8.0; flash energy ~3 μJ cm^{-2} at 680 nm, average of 256 repetitions at 10 Hz. Curve 1, carbon ink reference, 25 °C; curve 2, PS I trimer complexes without any addition with saturation background light, 25 °C; curve 3, carbon ink reference, 3.7 °C; curve 4, PS I trimer complexes, 60 μM PMS, 2 mM Asc, 25 °C; curve 5, PS I trimer complexes, 60 μM PMS, 2 mM Asc, 3.7 °C.

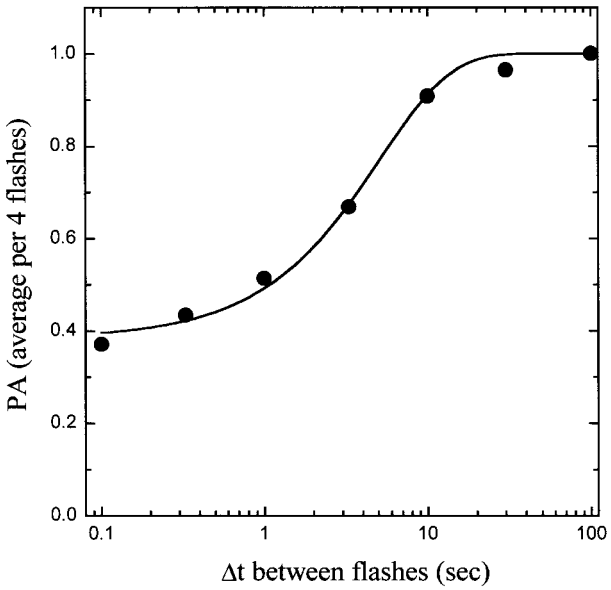

FIGURE 2: Recovery time of PS I trimer complexes at 3.7 °C: 10 mM Hepes, pH 8.0, 0.03% DM, 0.2 mM TMPD, 2 mM Asc, OD_{680} = 0.18/mm. See Table 1 for data and the Theory section for details of calculation method.

tion. The negative signal at 25 °C also implies that the enthalpy change of PS I photochemistry is small (see below).

Recovery Time. The recovery time of reaction centers is of importance in general and in particular for precise PA measurements. Using the PA technique one can easily measure the recovery time of PS I (Figure 2 and Table 1; for details see the Theory section). The recovery time of PS I is determined by the concentration of exogenous donor to P_{700}^+ (*5*). Using our pulsed PA techniques the time constant for the turnover of the system in the presence of DCIP (0.2 mM) and Asc (2 mM) at 4 °C is determined to be about 0.6 s. The direct donation to P_{700}^+ from reduced DCIP was reported to be 200 ms and 2s by monitoring near-IR absorbance changes (*36*). We found that PMS (60 μM PMS and 2 mM Asc) is a fast donor to PS I P_{700}^+ with a time constant less than 100 ms (Table 1), which is consistent with the time constant of ~3 ms for donation to P_{700}^+ from reduced PMS at 4 °C (*36*). The recovery time using 0.1−0.2 mM DAD and TMPD with 1−2 mM Asc as donors to PS I is about 5 s, indicating that DAD and TMPD are slow electron donors to P_{700}^+. To increase signal to noise, repetition of the PA measurement is required, but a flash interval shorter than the recovery time introduces error and a slower rate wastes time. On the basis of our results, with DAD or TMPD as donor for PS I, 0.1 Hz is appropriate, while with DCIP we can use 1 Hz.

Table 1: Recovery Time of PS I Trimer Complexes from *Synechocystis* 6803 in the Presence of Different Artificial Electron Donors at 4 °C[a]

donor	τ, s	fractions of fast and slow (τ) components: $a/(1-a)$
0.2 mM DAD + 2 mM Asc	6.3	0/1
0.2 mM TMPD + 2 mM Asc	5.0	0.18/0.82
0.2 mM DCIP + 2 mM Asc	0.6	0.21/0.79
60 μM PMS + 2 mM Asc	<0.1	1/0

[a] 10 mM Hepes, pH 8.0, 0.03% DM. Data were fitted to the following equation using the average: $PA = PA_0[a + (1-a)(1 - e^{-\Delta t/\tau})]$, where a = fraction of fast unresolved kinetic component and Δt = interval between flashes.

It should be noted that the recovery time is dependent on the excitation energy and temperature. Low excitation energy pulses will make the effective recovery time faster since only a random fraction of centers are hit with each flash. Higher temperature than 4 °C will also make the recovery time faster. Therefore, the recovery time reported here should be considered the largest value under our experimental conditions.

Volume Contraction. Upon excitation by light, charge separation takes place via electron transfer from the excited-state P_{700}* to the primary electron acceptor A_0 within some 10 ps. The electron is further transferred to A_1 and then to F_A/F_B iron−sulfur centers in less than 1 μs. These photochemical electron-transfer reactions lead to volume and enthalpy changes which are measured by PTRPA.

There are two different ways to obtain the volume change of the reaction centers: (1) low-energy yield method and (2) saturation method (see Theory section for detail). As shown in Figure 3, increasing the excitation energy of the flash causes a decrease in yield of negative volume change because of multiple excitations of the centers (*38*, *39*). In this case one can use the lowest energy of the flash to obtain the precise value of volume change times quantum yield. Unfortunately, this measurement has the problem of low signal to noise. To get more reliable results, we use curve fitting to eq 8 to obtain the limiting volume change of the samples. The results are listed in Table 2 as ΔV_y, which shows that with different donor systems we obtained identical values of volume contraction of PS I, -25 ± 2 Å^3 per center.

Alternatively, as in Figure 4, by fitting the curve via eq 9 we can obtain the maximum volume change independent of quantum yield, which is the total volume contraction of all PS I in the sample. This volume change of PS I is listed in Table 2 as ΔV_s.

These two different methods give the same value of volume change of PS I, -26 ± 2 Å^3. This implies that the quantum yield (Φ) is in fact unity. By use of pulsed photo-

Table 2: Photochemical and Thermodynamic Parameters of PS I Trimer Complexes from *Synechocystis* 6803

donor[a]	λ_{ex}, nm	$\Phi\sigma$, Å^2	Φ,[b] %	ΔV_y,[c] Å^3	ΔV_s,[d] Å^3	TE_0, %	ΔH, eV	$T\Delta S$,[e] eV
TMPD/Asc	680	220 ± 25	113 ± 15	−28 ± 3	−24 ± 3	71 ± 7	−0.51 ± 0.13	+0.23 ± 0.13
PMS/Asc	680	180 ± 18	92 ± 9	−26 ± 2		82 ± 4	−0.32 ± 0.07	+0.42 ± 0.07
DCIP/Asc	680			−26 ± 2	−24 ± 2	83 ± 4	−0.30 ± 0.07	+0.44 ± 0.07
PMS/Asc	625	47 ± 5	104 ± 10	−24 ± 2	−24 ± 2	80 ± 4	−0.35 ± 0.07	+0.39 ± 0.07
PMS/Asc	625	37 ± 6	82 ± 12	−22 ± 4	−27 ± 3	72 ± 6	−0.50 ± 0.10	+0.24 ± 0.10
PMS/Asc	680	170 ± 17	87 ± 9	−27 ± 2	−27 ± 2	81 ± 3	−0.34 ± 0.05	+0.40 ± 0.05
average			96 ± 11	−25 ± 2	−26 ± 2	78 ± 5	−0.39 ± 0.09	+0.35 ± 0.09

[a] pH 8.0, 10 mM Hepes, 0.03% DM. The concentrations of donors are as follows: 0.2 mM TMPD, 60 μM PMS, 0.2 mM DCIP, and 2 mM Asc. [b] The values are obtained from the ratio of calculated optical cross sections of PS I, 195 Å^2 and 45 Å^2 at 680 and 625 nm, respectively, to the effective optical cross sections $\Phi\sigma$. [c] The limiting value of the low-energy yield curve fit at 4 °C using eq 8. [d] The maximum PA signal at 4 °C when all reaction centers are excited (from eq 9). [e] ΔG is estimated to be −0.74 eV (from data in refs *4* and *48*−*53*).

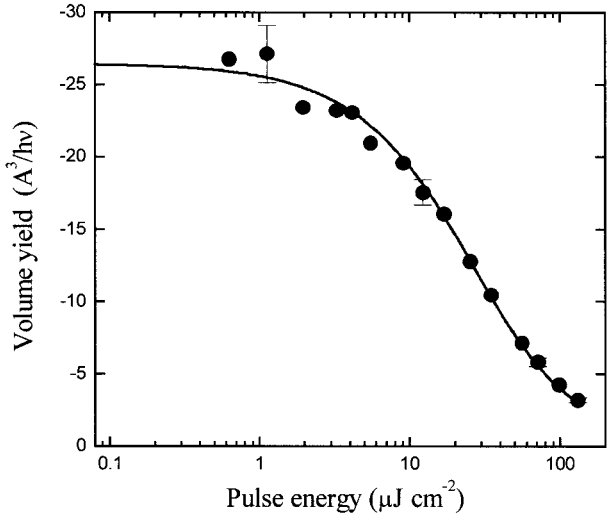

FIGURE 3: Volume yield of PS I trimer complexes at 680 nm and 3.7 °C: 10 mM Hepes, pH 8.0, 0.03% DM, 60 μM PMS, 2 mM Asc; OD_{680} = 0.166/mm. The excitation area of the sample within the PA cell is 1.33 cm^2. The fit is $\Delta V/E = \Delta V_y(1 - e^{-\Phi\sigma E})/(\sigma E)$ with $\Phi\sigma = 188 \pm 15$ Å^2 and $\Delta V_y = -27 \pm 2$ Å^3.

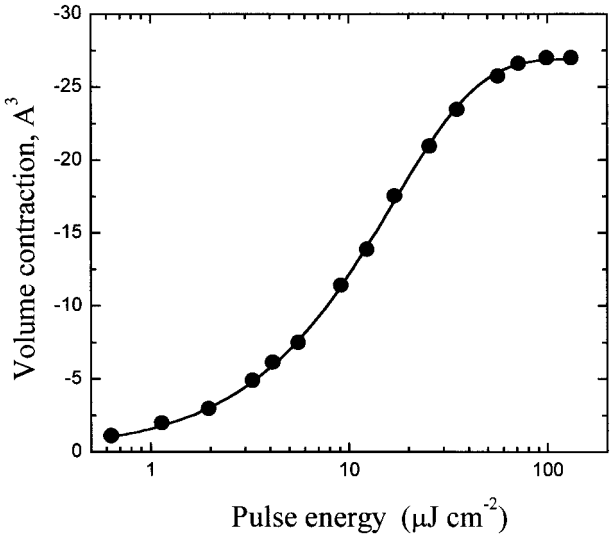

FIGURE 4: Saturation curve of PS I trimer complex volume contraction at 680 nm and 3.7 °C. The fit is $\Delta V = N\Delta V_s(1 - e^{-\Phi\sigma E})$ with $\Phi\sigma = 170 \pm 15$ Å^2 and $\Delta V_s = -26 \pm 2$ Å^3. Other conditions are the same as in Figure 3.

acoustics we will measure this important parameter as follows.

Quantum Yield of Photochemistry. Since the PA measurement determines the actual heat or volume change, i.e., the molar enthalpy or volume times the quantum yield, the latter must be known to obtain the molar quantities. Although some preliminary measurements of the quantum yield of PS I (*37*) are available, the precise value is unknown. The light saturation curve at 4 °C contains the information of interest (see Theory section). First, the optical cross section, σ, with units of area per reaction center, can be calculated from the absolute absorption spectra of the sample, the Chl content, and ratio of Chl to the primary electron donor P_{700}. Taking 6.4×10^4 mM^{-1} cm^{-1} as the extinction coefficient of Chl in situ at 680 nm (*33*) and the measured ratio of Chl to P_{700} of 80, the theoretical optical cross section (σ) was found to be 195 Å^2 per reaction center. The next step is to measure the effective optical cross section via the light saturation curve. Our flash energy E is uniform and constant cross the sample, and our sample is optically thin with $A \leq 0.1-0.2$. The effective cross section ($\phi\sigma$) was obtained by fitting the experimental light saturation curve (eq 9 and Figure 4). The quantum yield (Φ) of photochemistry in PS I antenna−reaction center complexes so determined with five independent measurements was found to be 96 ± 11% (Table 2).

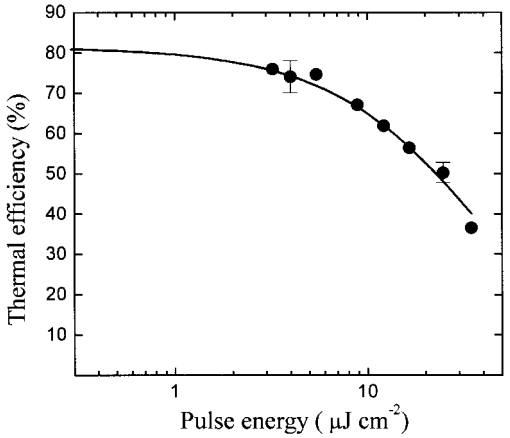

FIGURE 5: Thermal efficiency of PS I trimer complexes at 680 nm and 25 °C. The fit is $TE/E = TE_0(1 - e^{-\Phi\sigma E})/(\sigma E)$ with $\Phi\sigma = 155 \pm 15$ Å^2 and $TE_0 = 81 \pm 3\%$. Other conditions are the same as in Figure 3.

Thermal Efficiency and Reaction Enthalpy. One can obtain the efficiency and enthalpy via eqs 10 and 11. The absolute PA signal is dependent on the energy of the laser flash. Higher energy produces better signal-to-noise ratio, unfortunately with a lower efficiency because of saturation (Figure 5). For example, using energy of 15 μJ/cm^2 one obtains 60% efficiency instead of the limiting 80%. To address this problem, we use a curve-fitting method via eq 12 and are

Table 3: Comparison of Results of Global Convolution and Peak-to-Peak PA Data Analysis for the PS I Trimer Complex[a]

method	ΔV_y, Å^3	TE, %	ΔH, eV	$T\Delta S$, eV
global analysis	-25 ± 2	79 ± 5	-0.37 ± 0.09	$+0.37 \pm 0.09$
peak-to-peak analysis	-26 ± 2	78 ± 5	-0.39 ± 0.09	$+0.35 \pm 0.09$

[a] pH 8.0, 10 mM Hepes, 0.03% DM, 60 μM PMS, 2 mM Asc. The excitation wavelength is 680 nm.

able to obtain the limiting efficiency $TE_0 = 78 \pm 5\%$ and $\Delta H = -0.39 \pm 0.09$ eV (Figure 5 and Table 2).

To confirm our results, we used a global convolution analysis of PA data at all the different temperatures between 4 and 25 °C. The peak-to-peak analysis includes a noise level of up to 5%, while global analysis uses all of the points (500) of the curve, increasing the signal-to-noise ratio. These two different methods give similar (±8%) results (Table 3), indicating our results are reliable.

DISCUSSION

Assignment of the Electron-Transfer Reaction. PS I is a pigment−protein complex of at least 11 polypeptides embedded in the photosynthetic membranes of oxygenic photosynthetic systems. Absorption of light causes electron transfer from reduced plastocyanin (or cytochrome c_6) to oxidized ferredoxin (or flavodoxin) to generate NADPH (*5*, *6*).

According to known kinetic data (*4*, *40*−*46*), the electron-transfer steps in PS I reaction centers of *Synechocystis* 6803 include the light-induced charge separation and the subsequent electron transfer to secondary electron acceptors:

$$P_{700}{*}A_0A_1F_XF_A/F_B \xrightarrow{3-14\ ps} P_{700}{}^{+}A_0{}^{-}A_1F_XF_A/F_B \xrightarrow{20-50\ ps} P_{700}{}^{+}A_0A_1{}^{-}F_XF_A/F_B \xrightarrow{\sim 200\ ns} P_{700}{}^{+}A_0A_1F_X{}^{-}F_A/F_B \xrightarrow{50-200\ ns} P_{700}{}^{+}A_0A_1F_XF_A/F_B{}^{-}$$

After excitation of P_{700}, the charge separation for the formation of the radical pair $P_{700}{}^{+}A_0{}^{-}$ occurs in several picoseconds, and the electron is then transferred to A_1 from A_0 with a time constant of 20−50 ps (*41*). Then $A_1{}^{-}$ transfers an electron to F_X in about 200 ns. The detailed pathway and kinetics of electron transfer between F_X, F_A, and F_B had not yet been established. Recent studies using time-resolved absorption, time-resolved photovoltage, and EPR spectroscopies showed that F_A is proximal to P_{700} and favors a linear electron-transfer pathway $F_X \rightarrow F_A \rightarrow F_B \rightarrow$ ferredoxin (*42*−*45*). It is proposed that the electron transfers from F_X to F_A in about ∼50 ns and further to F_B with a time constant of ∼200 ns. Although the pathways of electron transfer between these three iron−sulfur clusters are not yet clear, the rate of electron transfer is agreed to be on the submicrosecond scale (*4*, *40*, *46*). Therefore, on the 1 μs time range, the final radical state monitored in our experiments is $P_{700}{}^{+}F_A/F_B{}^{-}$. The F_A/F_B pair may well be present in equilibrium amounts.

Different donor systems affect the recovery time of PS I reaction centers. In this paper four different artificial electron donors, DAD, DCIP, TMPD, and PMS, were tested (Table 1). Selection of the frequency of the laser flash (0.1−10 Hz) allows recovery of the reaction center in the presence of different donor systems upon excitation by repetitive laser flashes.

Volume Contraction. Charge separation of reaction centers induces a volume contraction via electrostriction. Although there may be other small contributions to this volume change (*59*−*62*), the magnitude of the changes points to electrostriction. This volume contraction is related directly to charge separation and is an ideal and absolute indicator of electron transfer. Optical measures of charge separation depend on interpretation of spectral signatures.

To certify the value of the volume change of PS I reaction centers, two methods of data analyses were used, i.e., yield method and saturation method. These two different methods give us the same volume change value within an error of 8% (Table 2), suggesting that our data are reliable. The former depends on the quantum yield and the latter does not, implying that the yield is unity.

We directly determined the quantum yield of primary charge separation in the reaction center using the measured and calculated optical cross sections (see Results). With five independent measurements, we found that this parameter is $96 \pm 11\%$ (Table 2). This finding allows our conclusion that the volume contraction in PS I of *Synechocystis* 6803 on the 1 μs time scale is -26 ± 2 Å^3. These parameters are discussed relative to those in PS II in the following paper (*58*).

Our value is somewhat larger than that reported for the isolated PS I reaction center from *Synechocystis* 6803 by Delosme et al. (*26*), about −20 Å^3. One reason could be the neglect of the change in compressibility κ of water in the range of 4−25 °C by these authors. Calculation without correction of κ would give a 10% less volume change.

Enthalpy. Although of equal importance, the thermodynamic properties of electron transfer, aside from the free energy, have been largely neglected in comparison with that of their kinetics. Furthermore, previous studies of the thermodynamics used mainly indirect techniques, such as delayed luminescence measurements along with changes in temperature. The data using these techniques may include some untested assumptions and components not accounted for by the simple theoretical analysis. Thus these early data should be considered as only preliminary.

The pulsed, time-resolved photoacoustic methodology that we have developed on the nanosecond to microsecond time scale has proven to be suitable for investigation of the thermodynamics of photosynthetic systems (*32*). By use of this method we have successfully measured the ΔV, ΔH, and $T\Delta S$ of electron transfer in aqueous solutions (*31*) and in purple bacterial reaction centers of *Rb*. *sphaeroides* (*32*). In this paper using PTRPA we found that the thermal efficiency (TE) of PS I on the 1 μs time scale is $78 \pm 5\%$ (Table 2). Further support is provided by the comparison of results of peak-to-peak and global analysis methods, which give identical values of the efficiency (Table 3). It is 40% on the millisecond time scale (*16*, *17*). The TE (∼80%) of PS I from *Synechocystis* 6803 here (Figure 5) is unexpectedly large.

Taking the quantum yield of photochemistry in PS I as unity, it is concluded that the enthalpy change for the formation of $P_{700}{}^{+}F_A/F_B{}^{-}$ from $P_{700}{*}$ is −0.39 eV (Table 2).

Entropy. A standard electron-transfer theory has been established (*28*). However, there are still some assumptions

that remain to be tested. For example, in theoretical calculations it has been assumed that the entropy of electron transfer is zero (*47*). Also the free energy of electron transfer is assumed to be independent of temperature (*29*, *30*). Recent kinetic and thermodynamic studies have shown that these assumptions may be not true (*10*, *31*, *32*). Using PTRPA the enthalpy and entropy of electron transfer from the triplet state of the electron donor zinc uroporphyrin to the electron acceptor naphthoquinone-2-sulfonate were determined in aqueous solutions (*31*). The entropy, $T\Delta S$ (T is 25 °C), of the above electron-transfer reaction is quite large and negative, −0.58 eV. A study of the bacterial reaction center of *Rb. sphaeroides* revealed a significant positive entropy change (+0.4 eV) for the formation of $P_{870}{}^{+}Q_A{}^{-}$ from the excited state P_{870}* (*32*).

In this study we extend our studies to oxygenic photosynthetic PS I reaction centers from *Synechocystis* 6803. We obtained the enthalpy for the formation of the radical pair of $P_{700}{}^{+}F_A/F_B{}^{-}$ from the excited-state P_{700}* as −0.39 eV. Free energy ΔG was calculated from the published values of redox midpoint potentials of cofactors in situ. Using the redox potentials of the cofactors $P_{700}{}^{+}/P_{700}$, +0.47 ± 0.02 V (*4*, *48*, *49*), and $F_{A,B}/F_{A,B}{}^{-}$, −0.56 ± 0.03 V (*50*−*53*), and P_{700}* energy (1.77 eV), we obtain $\Delta G = -0.74 \pm 0.05$ eV. By the thermodynamic relation $\Delta G = \Delta H - T\Delta S$ we obtain $T\Delta S$ of +0.35 ± 0.1 eV (Table 2). We refer to this as an apparent entropy since the free energy may be different in an unrelaxed state of the protein (*32*). This is close to the entropy (+0.4 eV) of reaction for formation of $P^{+}Q_A{}^{-}$ from the excited reaction centers of *Rb. sphaeroides* (*32*).

The PsaA and PsaB subunits of PS I form the heterodimeric core of the complex. The X-ray structure of cyanobacterial PS I revealed 11 transmembrane helices in both PsaA and PsaB (*7*). The recent three-dimensional structure of the PS II dimeric reaction center from higher plants at 8 Å resolution shows the similarity between PS I and PS II or bacterial reaction centers (*54*). The 7−11 transmembrane helices of PsaA and PsaB are analogous to D1 and D2 subunits, i.e., to L and M subunits of bacterial reaction centers. The structure of the bacterial reaction center from *Rb. sphaeroides* shows a net negative charge on the P_{870} side and a net positive charge on the Q_A side (*55*). Taking the 7−11 transmembrane helices of PsaA and PsaB sequences from *Synechocystis* 6803 and the folding model of PsaA and PsaB in PS I proposed by Sun et al. (*56*), we calculate the charges for PS I on both sides of the membrane. This shows that there are excess charges (+13) on the A_1 side and (−1) on the P_{700} side of membranes, respectively (Table 4). These charges in the PS I reaction center, as in the bacterial reaction center, favor the electron transfer through the membrane. Bound counterions are expected to accompany these excess charges, at least on the A_1 side, because of the long distance between the interfaces. The transmembrane electron transfer would cancel one each of these excess charges and thus liberate counterions. Similar to reaction centers of *Rb. sphaeroides* (*32*), we propose that the unexpected sign of entropy of electron transfer in PS I is attributed to the escape of the counterions from the surface of the particles.

An alternative interpretation of these results (*32*) is that the free energy of the reaction is much less at the short time scale of the electron transfer (approximately nanosecond); i.e., the free energy of the ion pair is larger and decreases to that of the measured potentials only on a time scale greater than microseconds by dielectric relaxation in the protein. However, to obtain a change in free energy of 0.4 eV, the effective dielectric coefficient of the protein would have to approximately double, assuming Born charging energy of the ions. This is unlikely. Moreover, the discrepancy in free energy and enthalpy in PS II is smaller and of opposite sign (*58*). The volume contraction in PS II is also much smaller, possibly involving proton movement.

Table 4: Charges on the A_1 and P_{700} Sides of the Membrane in PS I from *Synechocystis* 6803[a]

protein sequences of PsaA and PsaB	charges		
	positive[b]	negative[c]	net
A_1 side	(+34)	(−21)	(+13)
B394−B414	+5	−5	0
B533−B571	+6	−6	0
B663−B703	+7	−3	+4
A412−A433	+6	−3	+3
A551−A588	+6	−2	+4
A688−A723	+4	0	+4
P_{700} side	(+15)	(−16)	(−1)
B438−B513	+2	−7	−5
B594−B639	+3	−2	+1
B719−B731	+1	0	+1
A458−A530	+5	−4	+1
A612−A663	+3	−3	0
A745−A751	+1	0	+1

[a] Calculation is based on the folding model of PS I core proteins PsaA and PsaB from ref *56*. [b] Positive charges are calculated as the numbers of the lysine, arginine, and histidine residues. [c] Negative charges are the numbers of aspartic acid and glutamic acid residues.

Our in vivo measurements in the whole cells of *Synechocystis* (*57*) have revealed ΔV of −27 Å^3, ΔH of −0.33 eV, and $T\Delta S$ of +0.4 eV for the primary reaction in PS I that is in good agreement with the in vitro data. In contrast to these properties of PS I and bacterial reaction centers, our results on PS II core complexes show significantly smaller volume contraction and a negative entropy (*57*, *58*).

CONCLUSION

Using the PTRPA technique, we obtained the thermodynamic data for charge transfer in PS I reaction centers from the cyanobacterium *Synechocystis* sp. PCC 6803 on the 1 μs time scale. Volume contraction from the light-induced charge separation forming $P_{700}{}^{+}F_A/F_B{}^{-}$ in PS I is −26 ± 2 Å^3. The enthalpy of the above electron-transfer reaction in PS I is −0.39 ± 0.1 eV. These data allow us to calculate a significant entropy change for this reaction, $T\Delta S = +0.35 \pm 0.1$ eV. Thus the volume change, the enthalpy, and the entropy of the electron-transfer reaction are similar to those of the bacterial reaction center (*32*).

ACKNOWLEDGMENT

We are grateful to John Golbeck for valuable information of Fe_4S_4 clusters and to Kai Sun and Greg Edens for insightful discussions. We thank Irene Zielinski-Large for very able technical assistance.

REFERENCES

1. Deisenhofer, J., and Norris, J. R., Eds. (1993) *The Photosynthetic Reaction Center*, Vols. I and II, Academic Press, Inc., San Diego.

2. Ort, D., and Yocum, C. F., Eds. (1996) *Oxygenic Photosynthesis*: *The Light Reactions*, Kluwer Academic Publishers, Dordrecht, The Netherlands.
3. van Grondelle, R., Dekker, J. P., Gillbro, T., and Sundstrom, V. (1994) *Biochim. Biophys. Acta 1187*, 1−65.
4. Brettel, K. (1997) *Biochim. Biophys. Acta 1318*, 322−373.
5. Golbeck, J. H. (1994) in *The Molecular Biology of Cyanobacteria* (Bryant, D. A., Ed.) pp 319−360, Kluwer Academic Publishers, Dordrecht, The Netherlands.
6. Chitnis, P. R. (1996) *Plant Physiol. 111*, 661−669.
7. Krauss, N., Schubert, W.-D., Klukas, O., Fromme, P., Witt, H. T., and Saenger, W. (1996) *Nat. Struct. Biol. 3*, 965−969.
8. Hervas, M., Mavarro, J. A., Diaz, A., and De la Rosa, M. A. (1996) *Biochemistry 35*, 2693−2698.
9. van Gorkom, H. J. (1985) *Photosynth. Res. 6*, 97−112.
10. Woobury, N. W., and Allen, J. P. (1995) in *Anoxygenic Photosynthetic Bacteria* (Blankenship, R. E., Madigan, M. T., and Bauer, C. E., Eds.) pp 527−557, Kluwer Academic Publishers, Dordrecht, The Netherlands.
11. Mauzerall, D., Gunner, M. R., and Zhang, J. W. (1995) *Biophys. J. 68*, 275−280.
12. Mauzerall, D., Feitelson, J., and Prince, R. (1995) *J. Phys. Chem. 99*, 1090−1093.
13. Malkin, S. (1996) in *Biophysical Techniques in Photosynthesis* (Amez, J., and Hoff, A. J., Eds.) pp 191−206, Kluwer Academic Publishers, Dordrecht, The Netherlands.
14. Canaani, O., Malkin, S., and Mauzerall, D. (1988) *Proc. Natl. Acad. Sci. U.S.A. 85*, 4725−4729.
15. Mauzerall, D. (1990) *Plant Physiol. 94*, 278−283.
16. Cha, Y., and Mauzerall, D. (1992) *Plant Physiol. 100*, 1869−1877.
17. Charlebois, D., and Mauzerall, D. (1999) *Photosynth. Res. 59*, 27−38.
18. Braslavsky, S. E., and Heibel, G. E. (1992) *Chem. Rev. 92*, 1381−1410.
19. Fork, D. C., and Herbert, S. K. (1993) *Photochem. Photobiol. 57*, 207−220.
20. Feitelson, J., and Mauzerall, D. (1993) *J. Phys. Chem. 97*, 8410−8413.
21. McLean, M. A., Di Primo, C., Deprez, E., Bon Hoa, G. H., and Sligar, S. G. (1998) *Methods Enzymol. 295*, 316−330.
22. Zhang, D., and Mauzerall, D. (1996) *Biophys. J. 71*, 381−388.
23. Arata, H., and Parson, W. (1981) *Biochim. Biophys. Acta 636*, 70−81.
24. Malkin, S., Churio, M. S., Shochat, S., and Braslavsky, S. E. (1994) *J. Photochem. Photobiol. 23B*, 79−85.
25. Puchenkov, O. V., Kopf, Z., and Malkin, S. (1995) *Biochim. Biophys. Acta 1231*, 197−212.
26. Delosme, R., Beal, D., and Joliot, P. (1994) *Biochim. Biophys. Acta 1185*, 56−64.
27. Nitsch, C., Braslavsky, S. E., and Schatz, G. H. (1988) *Biochim. Biophys. Acta 934*, 201−212.
28. Marcus, R. A., and Sutin, N. (1985) *Biochim. Biophys. Acta 811*, 265−322.
29. Gunner, M. R., and Dutton, P. L. (1989) *J. Am. Chem. Soc. 111*, 3400−3412.
30. Moser, C. C., Keske, J. M., Azrncke, K., Farid, R. S., and Dutton, P. L. (1993) in *The Photosynthetic Reaction Center* (Deisenhofer, J., and Norris, J. R., Eds.) Vol. II, pp 1−22, Academic Press, Inc., San Diego.
31. Feitelson, J., and Mauzerall, D. (1996) *J. Phys. Chem. 100*, 7698−7703.
32. Edens, G. J., Gunner, M. R., Xu, Q., and Mauzerall, D. (2000) *J. Am. Chem. Soc. 122*, 1479−1485.
33. Sun, J., Ke, A., Jin, P., Chitnis, V. P., and Chitnis, P. R. (1998) *Methods Enzymol. 297*, 124−139.
34. Arnaut, L. G., Caldwell, R. A., Elbert, J. E., and Melton, L. A. (1992) *Rev. Sci. Instrum. 63*, 5381−5389.
35. Mauzerall, D. (1986) *Photosynth. Res. 10*, 163−170.
36. Vassiliev, I. R., Jung, Y.-S., Mamedov, M., Semenov, A. Yu., and Golbeck, J. H. (1997) *Biophys. J.* 72, 301−315.
37. Borisov, A. Yu., and Il'ina, M. D. (1973) *Biochim. Biophys. Acta 325*, 240−246.
38. Mauzerall, D. (1976) *Biophys. J. 16*, 87−91.
39. Mauzerall, D. (1979) *Photochem. Photobiol. 29*, 169−170.
40. Joliot, P., and Joliot, A. (1999) *Biochemistry 38*, 11130−11136.
41. Brettel, K., and Vos, M. H. (1999) *FEBS Lett. 447*, 315−317.
42. Diaz-Quintana, A., Leibl, W., Bottin, H., and Setif, P. (1998) *Biochemistry 37*, 3429−3439.
43. Mamedov, M. O., Grourovskaya, K. N., Vassiliev, I. R., Golbeck, J. H., and Semenov, A. Yu. (1998) *FEBS Lett. 431*, 219−223.
44. Lakashmi, K. V., Jung, Y.-S., Golbeck, G. H., and Brudvig, G. W. (1999) *Biochemistry 38*, 13210−13215.
45. Golbeck, J. H. (1999) *Photosynth. Res. 61*, 107−144.
46. Leible, W., Toupance, B., and Breton, J. (1995) *Biochemistry 34*, 10237−10244.
47. DeVault, D. (1980) *Q. Rev. Biophys. 13*, 387−564.
48. Setif, P., and Mathis, P. (1980) *Arch. Biochem. Biophys. 204*, 477−485.
49. Nugent, J. H. A. (1996) *Eur. J. Biochem. 237*, 519−531.
50. Ke, B., Hanson, R. E., and Beinert, H. (1973) *Proc. Natl. Acad. Sci. U.S.A. 70*, 2941−2945.
51. Cui, L. Y., Bingham, S. E., Kuhn, M., Kass, H., Lubitz, W., and Webber, A. N. (1995) *Biochemistry 34*, 1549−1558.
52. Jung, Y. S., and Golbeck, J. H. (1995) *Photosynth. Res. 46*, 249−255.
53. Evans, M. C. W., Reeves, S. G., and Cammack, R. (1974) *FEBS Lett. 49*, 111−114.
54. Rhee, K.-H., Morris, E. P., Barber, J., and Kuhlbrandt, W. (1998) *Nature 396*, 283−286.
55. Yeates, T. O., Komiya, H., Rees, D. C., Allen, J. P., and Feher, G. (1987) *Proc. Natl. Acad. Sci. U.S.A. 84*, 6438−6442.
56. Sun, J., Xu, Q., Chitnis, V. P., Jin, P., and Chitnis, P. R. (1997) *J. Biol. Chem. 272*, 21793−21802.
57. Boichenko, V. A., Hou, J.-M., and Mauzerall, D. (2001) *Biochemistry 40*, 7126−7132.
58. Hou, J.-M., Boichenko, V., Diner, B. A., and Mauzerall, D. (2001) *Biochemistry 40*, 7117−7125.
59. Borsarelli, C., and Braslavsky, S. E. (1998) *J. Phys. Chem. B 102*, 6231−6238.
60. Borsarelli, C., and Braslavsky, S. E. (1999) *J. Phys. Chem. A 103*, 1719−1727.
61. Losi, A., Braslavsky, S. E., Gartner, W., and Spudich, J. L. (1999) *Biophys. J. 76*, 2183−2191.
62. Wegewije, B., Paddon-Row, M. N., and Braslavsky, S. E. (1998) *J. Phys. Chem. A 102*, 8812−8818.

BI0103720